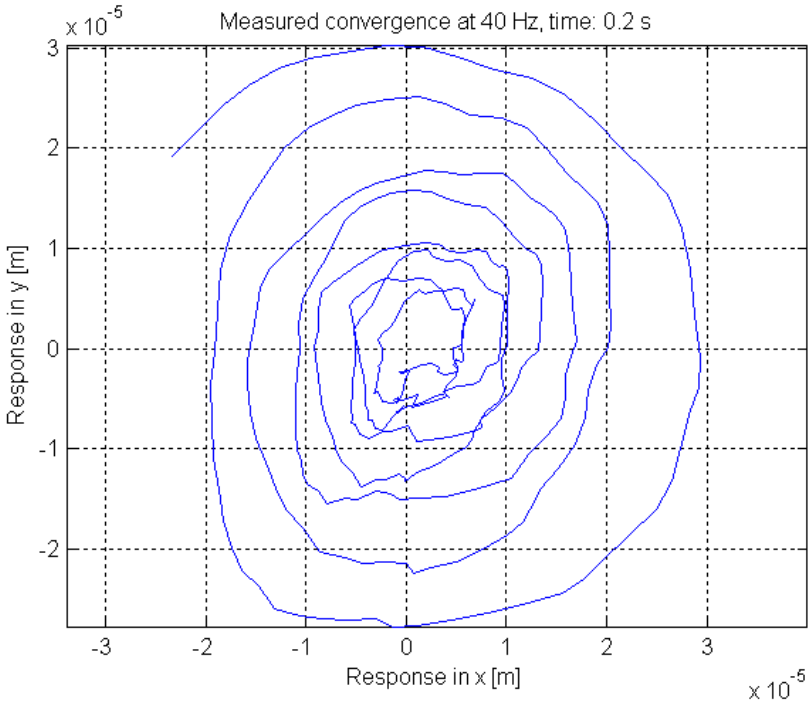

Mass Imbalance Compensation of Rotor with Adaptive Finite-Impulse-Response Filter and Convergent Control

Customer: VTT Industrial Systems

Public	X	Registered in VTT publications register JURE	X
Confidential until / permanently			
Internal use only			

Title

Mass Imbalance Compensation of Rotor with Adaptive Finite-Impulse-Response Filter and Convergent Control

Customer or financing body and order date/No.	Research report No.
VTT Industrial Systems	BTUO57-031122
Project	Project No.
T3SULARIPS	G3SU00104
Author	No. of pages/appendices
Kari Tammi	23 / 6

Keywords

active control, vibration, rotor, imbalance, adaptive filter, FIR, convergent control

Summary

This work introduces two principles to compensate a deterministic excitation from a system: adaptive finite impulse-response-filter and convergent control. Both principles work as adaptive feedforward compensation algorithms by feeding a compensation signal into the system. The compensation signal is generated from a reference signal that is correlated with the excitation to be compensated. The difference between the principles is the algorithm to derive the compensation signal from the reference signal. These algorithms are reported in the work. The methods were compared with simulations by compensating a sinusoidal disturbance in a simple plant. The convergent control algorithm indicated smoother but slower convergence than the adaptive finite impulse-response-filter with least-mean-square algorithm.

The convergent control was also tested in the rotor test environment. The displacement responses of the test rotor were measured when the convergent control was switched on. The measurements were carried out when the rotor was running 25 Hz, 40 Hz, and 65 Hz. The control force commands were also recorded at these speeds. The displacement response was also measured during a sweep from 11 Hz to 65 Hz. The convergent control was found working properly; the convergence of the algorithm was particularly fast. The performance of the algorithm may be improved by improving the quality of the compensation signal.

The forces used for control were low: from 1 N to 3 N. The parameter update seemed to have an effect on response; the response was slightly amplified at the update frequency.

Date 11 April, 2003

Pekka Koskinen
Deputy Research Manager

Kari Tammi
Research Scientist

Checked

Distribution (customers and VTT): Matti K. Hakala, Jussi Hyyryläinen, Markku Järviluoma, Pekka Koskinen, Kalervo Nevala, Ismo Vessonen

VTT TECHNICAL RESEARCH CENTRE OF FINLAND
VTT INDUSTRIAL SYSTEMS
Tekniikantie 12, Espoo
P.O. Box 1705, FIN-02044 VTT
FINLAND
Tel. +358 9 4561
Fax +358 9 455 0619
name.surname@vtt.fi
www.vtt.fi/tuo
Business ID 0244679-4

Table of contents

1 Introduction

This work was carried out for the project on active vibration control of rotors. The project belongs to the VTT research theme 'Intelligent Products and Systems'.

Compensation of a deterministic disturbance due to rotation is one of the challenges of active vibration control in rotating machines. Excitations induced by a rotating object, a rotor, are characterised by frequencies equal to the rotational frequency, and its multiples. Generally, the greatest excitation occurs at the rotational frequency. However, multiples of the rotational frequency may cause a significant response in the system if they meet a resonance frequency. The frequency, or the frequencies, of the major excitations are known because the rotational speed of a rotating machine is often measured. The key-idea of two compensation algorithms to be studied is to use a compensation signal generated from the rotational speed measurement and generate a control action that counter-acts with the excitation. The problem is to adjust such a gain and such a phase that the excitation is compensated. The adaptive finite-impulse-response (FIR) filter offers a solution by adapting the filter using the least-mean-squares algorithm. Second algorithm to be studied, the convergent control, applies an integrative update law on the Fourier coefficients of the compensation signal.

Figure 1 clarifies the idea. A vibrating system is located in the grey box. A harmonic disturbance at a known frequency is acting in the output. The objective is to feed such a compensation signal in the vibrating system that position remains zero. In other words, the algorithms adjust the gain and the phase of feedforward control such that the reference signal compensates the disturbance.

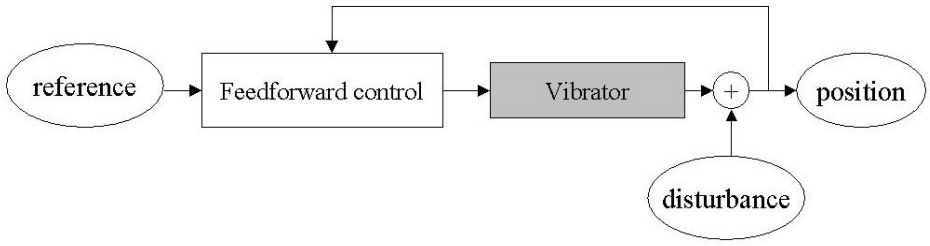

Figure 1. The compensation algorithms compensate the disturbance in the output by using the reference signal with the same frequency content but arbitrary amplitude and phase with respect to the disturbance.

This work was carried out as a comparative study on two adaptation principles to compensate a deterministic excitation from a system: adaptive finite impulse-response-filter and convergent control. The work is connected with the work by Tammi (2003). In the previous work, the velocity feedback control and the adaptive control based on adaptive finite-impulse-response filter were tested on the desktop test environment. The convergent control algorithm has been applied *e.g.* by Järviluoma & Valkonen (2001, 2002). Several algorithms for the compensation of a harmonic disturbance were reported by Järviluoma (2003).

This paper presents a comparative study between the adaptive FIR and the convergent control using simulations. Furthermore, the implementation and the tests of the convergent control algorithm in the desktop test environment are reported.

2 Materials & Methods

In this section, the test environment is described shortly and the adaptation principles are presented. For a more thorough discussion on the test environment, see Tammi (2003).

2.1 Test environment

The test environment was tailored to represent the Jeffcott rotor by locating the cylinder (diameter: 47.5 mm, length: 65 mm) in the middle of the slim shaft (diameter 10 mm, bearing span: 460 mm). The rotor was considered as two separate one-degree-of-freedom systems (Figure 2). One system was considered to vibrate in the horizontal (X) direction and the other system in the vertical (Y) direction. The actuating point of the force and the placement of the displacement transducer were approximately collocated (the transducers located 60 mm from the midpoint of the rotor).

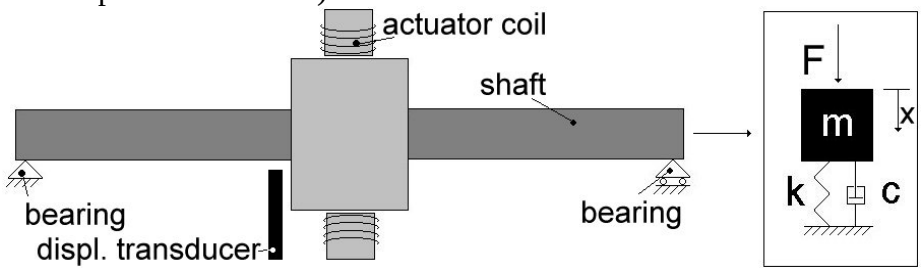

Figure 2. One direction of the rotor-actuator system was simplified to a one-degree-of-freedom vibrator. The other direction formed another similar system.

2.2 Adaptive FIR

The adaptive filter is presented in Fuller *et al.* (1996), for example. The notation was adopted from this textbook. The output of a finite-impulse-response filter (FIR) can be expressed as a convolution with the coefficients of the filter and the input signal. The output of the filter is equal to

$$u(n) = \sum_{i=0}^{I-1} h_i x(n-i), \tag{1}$$

where $x(n)$ is the input signal, I is the order of filter, and n is the index pointing to the latest pulse input, and n-i represents a shift backwards by i pieces. Thus, $u(n)$ is a sum of input pulses multiplied by the coefficients h_i. The error in the output can be described by

$$e(n) = d(n) + G(q)u(n), \tag{2}$$

where $d(n)$ is the disturbance and $G(q)$ is the system to be compensated. The error can be expressed as a function of the reference signal $x(n)$

$$e(n) = d(n) + G(q)H(q)x(n), \tag{3}$$

where $H(q)$ is the impulse response of the FIR filter. The order of $H(q)$ and $G(q)$ can be changed due they are linear and time invariant. After the modification, the error is

$$e(n) = d(n) + H(q)G(q)x(n). \tag{4}$$

The filtered reference signal is defined as

$$r(n) = G(q)x(n), \tag{5}$$

where the filtered reference signal $r(n)$ is obtained by filtering the original reference signal $x(n)$ through the model representing the mechanical system. The error in the output yields

$$e(n) = d(n) + \sum_{i=0}^{I-1} h_i r(n-i)\,. \tag{6}$$

The objective is to minimise the error in the output. A quadratic cost function for the error signal is equal to

$$J = e^2(n)\,, \tag{7}$$

where J is to be minimised. The update law for the coefficients is obtained with the gradient descent algorithm

$$h_i(n+1) = h_i(n) - \mu \frac{\partial J}{\partial h_i(n)}\,, \tag{8}$$

where μ is a convergence coefficient. From Equation (7), the derivative of the cost function can be written by using the partial derivative of the error with respect to the coefficients

$$\frac{\partial J}{\partial h_i(n)} = 2e(n)\frac{\partial e}{\partial h_i(n)}\,. \tag{9}$$

Finally, the update law for the filter coefficients can be expressed as

$$h_i(n+1) = h_i(n) - \alpha e(n) r(n-i)\,, \tag{10}$$

where α is another convergence coefficient ($\alpha = 2\mu$). The maximum value of the convergence coefficient is approximately

$$\alpha_{\max} \approx \frac{1}{r^2 I}\,. \tag{11}$$

The algorithm is known as the *filtered x-LMS algorithm* (Figure 3). (Vance 1996).

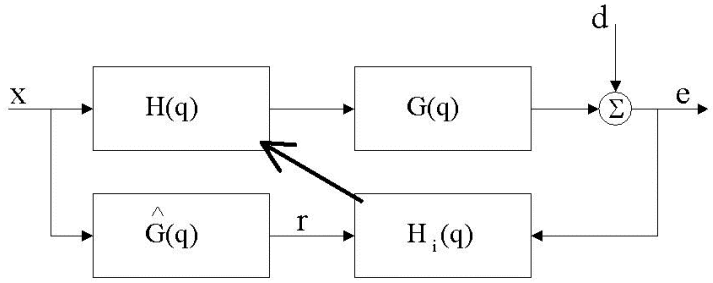

Figure 3. The block $G(q)$ represents the system to be damped. The reference signal is filtered in the model of the system $\hat{G}(q)$. The parameters of the filter are updated in block $H_i(q)$ and copied into the filter $H(q)$.

2.3 Convergent control

The principle of the convergent control algorithm was presented by Knospe *et al.* (1997). A similar control system, so called higher harmonic control was presented by Hall & Wereley (1989); and applied by Sievers & von Flotow (1988), for example. Modifications have also been made, see for example Lantto (1999).

The response of a rotor (at one frequency) can be expressed by using Fourier coefficients of the excitation and of the system frequency response

$$X_i = TU_i + X_{0i}, \tag{12}$$

where the X_i represent the vibration in the output of the system, T is the frequency response of the system, U_i is the input (open-loop control), and is X_{0i} the synchronous vibration due to rotation. The index *i* refers to the *i*th control step. The function to be minimised is chosen as

$$J = X_i^T X_i, \tag{13}$$

The adaptation law is obtained

$$U_{i+1} = U_i + AX_i, \tag{14}$$

where U_{i+1} is the control action in the next control period, U_i is the control action in the previous period, and A is the inverse of the system model. (Knospe *et al.* 1997, Sievers & von Flotow 1992). A very similar update law as for the FIR filter was derived. In order to achieve convergence, the inverse of the system model was multiplied with a convergence coefficient as in the case of FIR filter. By defining

$$A = -\frac{\alpha}{G(s)}, \tag{15}$$

where α is again a convergence coefficient and $G(s)$ is the model of the system. The algorithm converged by selecting a proper positive value for the convergence coefficient α. The computation of the Fourier coefficients was not explicitly specified by Knospe *et al.* (1997). They can be computed over a time interval respectively to the discrete Fourier transform. A simplified way is to compute them in each instant of time and use as such. In Figure 4, the coefficients are computed by multiplying the measured signal with complex signal (Sievers & von Flotow 1992, Lantto 1999).

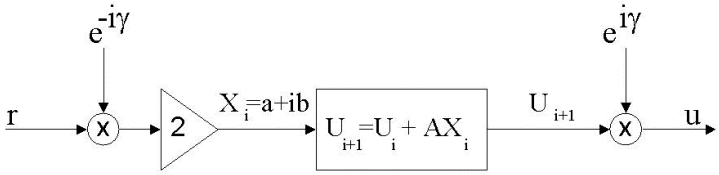

Figure 4. The real signal r is multiplied by the complex signal $e^{-i\gamma}$ and the control law is applied on the complex coefficients. The signal is then realised by multiplying with the complex conjugate signal.

3 Results

3.1 Comparison with simulations

In simulations, both systems were used to compensate a disturbance at one frequency in a simple vibrating system; see one-degree-of-freedom oscillator in Figure 2. The system was of second order having poles at -176 ± i 179 rad/s and the static gain of unity. The system had a well-damped resonance at 40 Hz.

The simulation models were built on Matlab Simulink; the models are shown in Appendix 1. The aim was to compensate one frequency in time and to compare the convergence of two algorithms. Both algorithms used the model of the actual system to be damped. In simulations, the model was the same as the system to be damped. The order of the adaptive

FIR was selected to 50. The maximum convergence coefficients were selected in such a way that the algorithms were stable in the frequency band from 10 Hz to 80 Hz. The trials led coefficients of 0.002 for the adaptive FIR and 0.02 for the convergent control.

The simulation results are presented at constant disturbance frequencies from 10 Hz to 80 Hz by 10 Hz steps. In Figure 5, the responses to 10 Hz and 20 Hz disturbances are shown. Figure 6 shows the convergence at 30 Hz and 40 Hz. From 10 Hz to 30 Hz, the rate of convergence grew together with the frequency of the disturbance. The responses at 50 Hz and 60 Hz are shown in Figure 7; and the responses at 70 Hz and 80 Hz are shown in Figure 8. The adaptive FIR filter had faster convergence up to 60 Hz than the convergent control. On other hand, the convergent control indicated smooth behaviour whereas the system with the adaptive FIR filter was vibrating during the convergence.

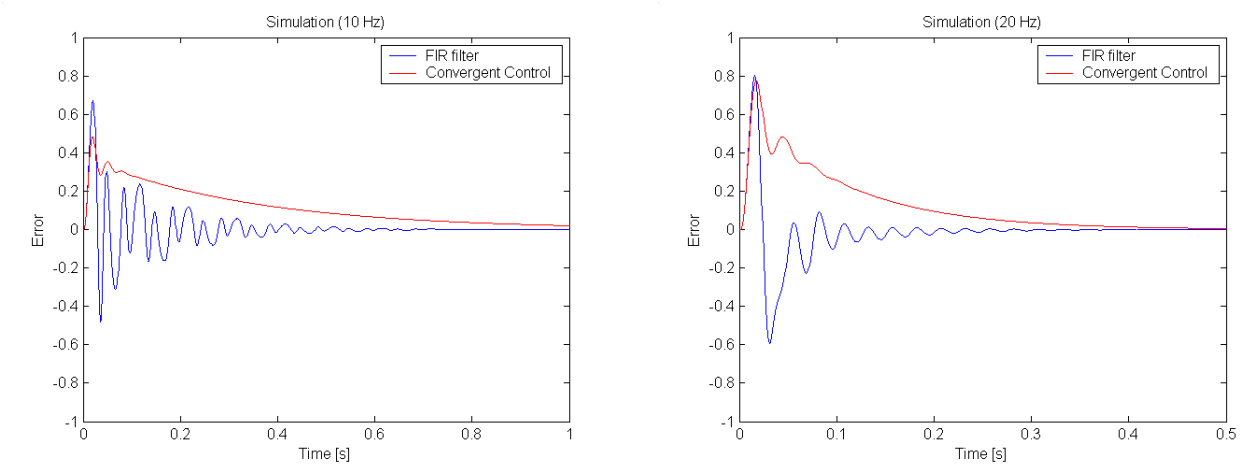

Figure 5. The convergence simulated with excitation of 10 Hz and 20 Hz. Note different time scales.

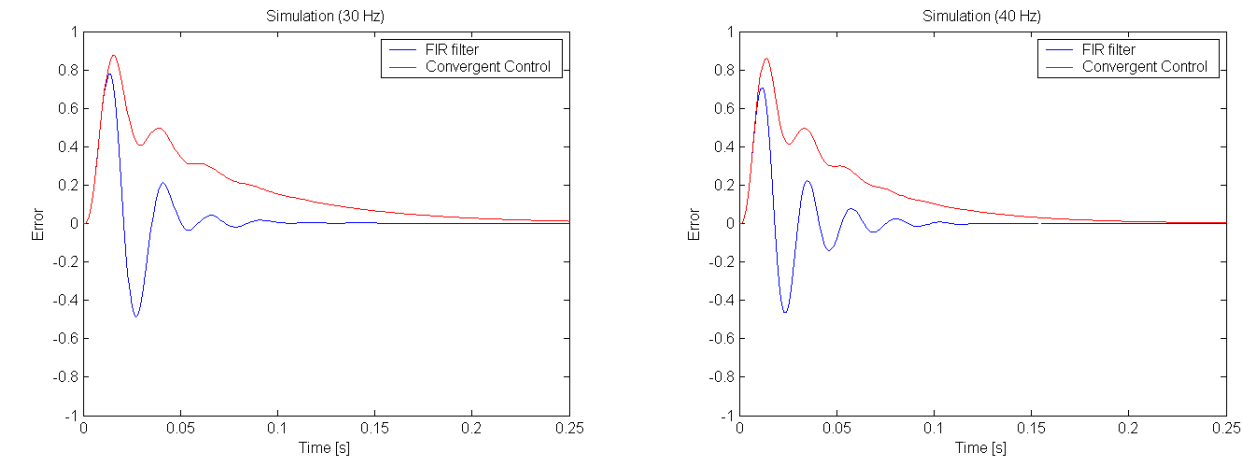

Figure 6. The convergence was simulated with 30 Hz and 40 Hz. The resonance of the system to be damped located at 40 Hz.

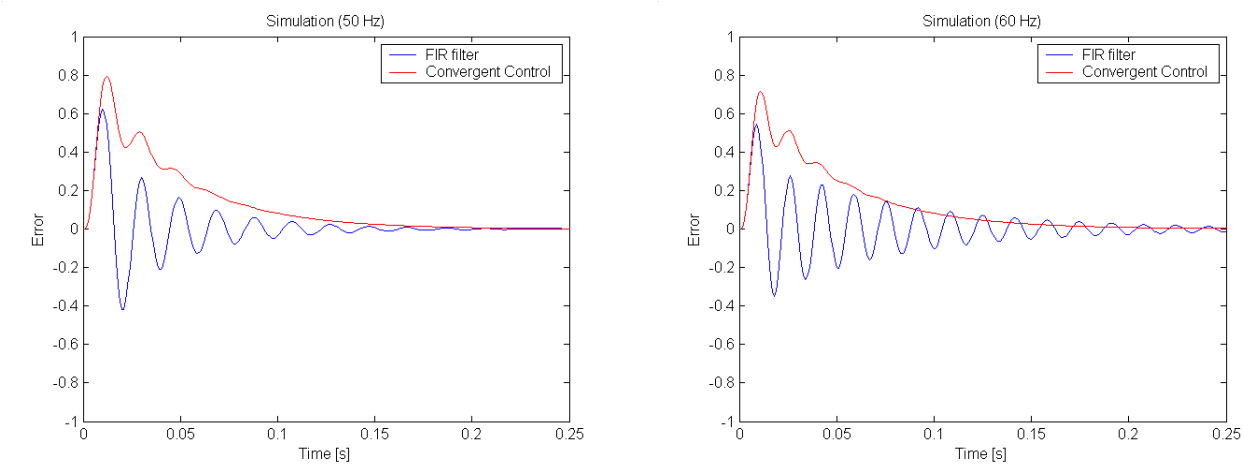

Figure 7. The vibrations of the adaptive FIR filter increased again at the frequencies above the resonance.

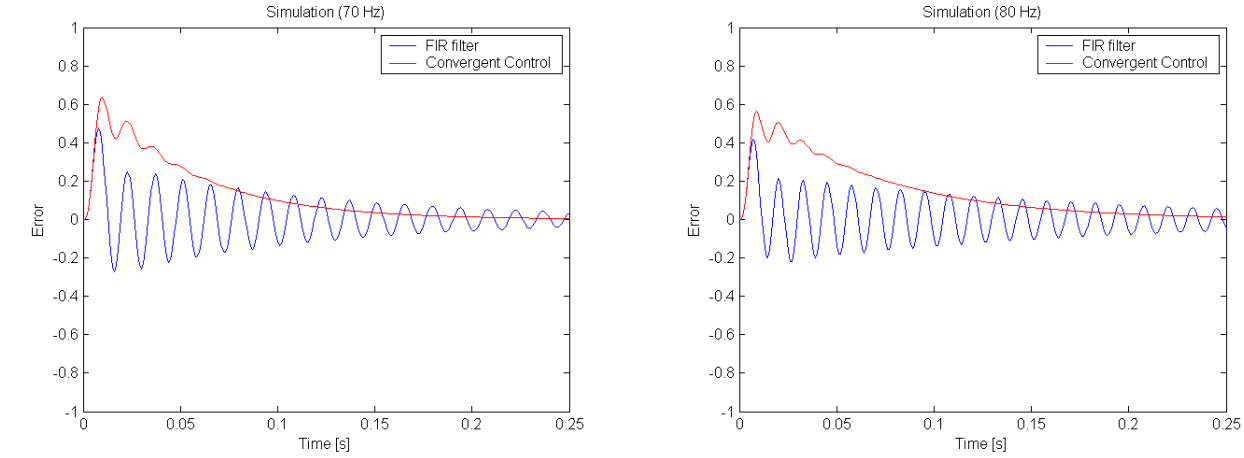

Figure 8. *The convergence simulated at 70 Hz and 80 Hz.*

3.2 Experiments with convergent control

The convergent control algorithm was implemented into the rotor test environment. The code can be found in Appendix 2 as it was programmed on the DSP[1] development environment. The tests and the test set-up corresponded to the ones carried out on the adaptive FIR filter and reported in Tammi (2003).

First, integration was used to compute the Fourier coefficients. When computing Fourier coefficients, different integration times were used from 0.01 s to 1 s. However, any advantages of integration were not observed and the feature was removed from the code. Note that this discussion only concerns the computation of the Fourier coefficients; the adaptation law in Equation (14) remained the same during the tests. Note also that the principle of the higher harmonic control is very similar with the principle used in this study.

[1] Digital Signal Processor

The convergence coefficient used in the tests was equal to 0.1. The value cannot directly be compared to the value used in the simulations due to the systems and the scaling of signals differ each other. In tests, the maximum stable value for the convergence coefficient was between 0.5 and 1.0. The output of the convergent control was updated every 100th control period (about every 0.01 seconds).

3.3 Displacement responses

In the tests, the displacement response of the system was measured by means of the eddy current transducers. The transducers were the very same as used by active control (see Figure 2). The data was sampled with a rate of 2048 Hz. Figure 9 shows the displacement response of the system when the algorithm was switched on; the rotational speed was 25 Hz (1500 rpm). In the beginning of the time record, feedback control was running alone the displacement being about 30 microns (peak). The convergent control algorithm was switched on and the response decreased to an order of two microns. The same procedure was repeated when the rotational speed was 40 Hz (2400 rpm) and 65 Hz (3900 rpm). The responses are shown in Figure 10 and Figure 11. The convergence was relatively fast; the steady-state condition was achieved in about 0.25 seconds. The amplitudes are approximately the same at different frequencies due to the velocity feedback control.

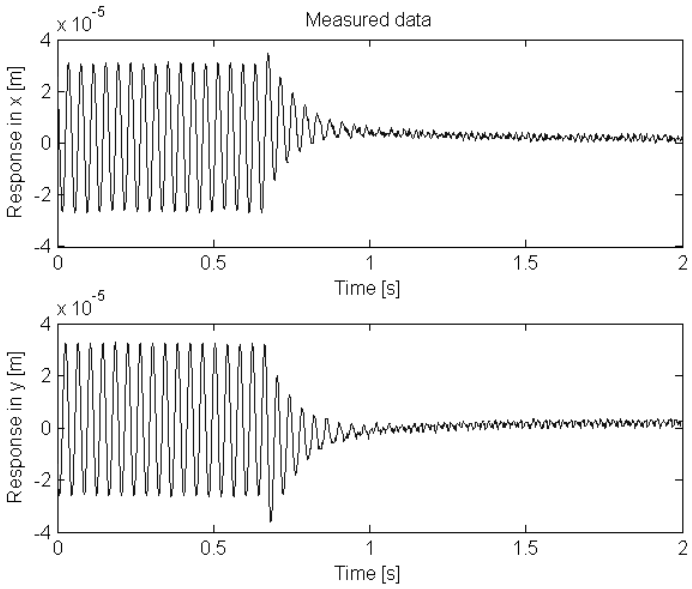

Figure 9. The feedback control was running alone until the convergent control was switched on (at about 0.6 seconds). The displacements were decreased from 30 microns to 2 microns after the switch-on. The rotational speed was 25 Hz.

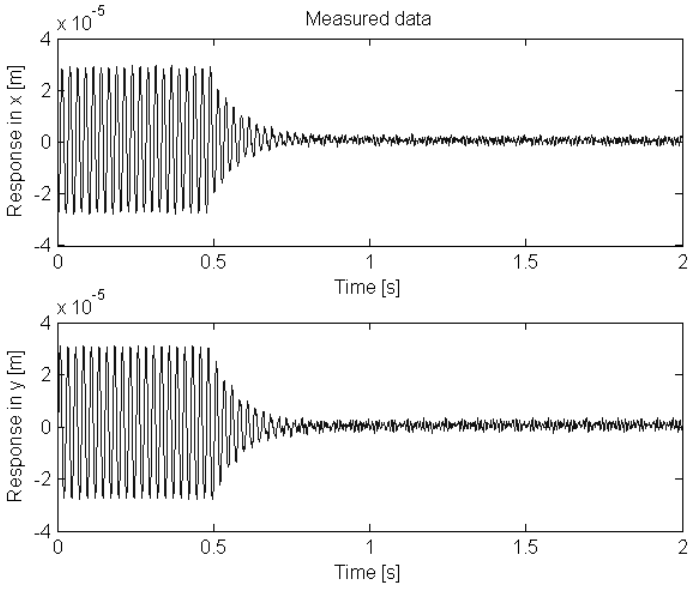

Figure 10. The responses were also measured during the switch-on of the convergent control when running at the critical speed of the rotor (40 Hz, 2400 rpm).

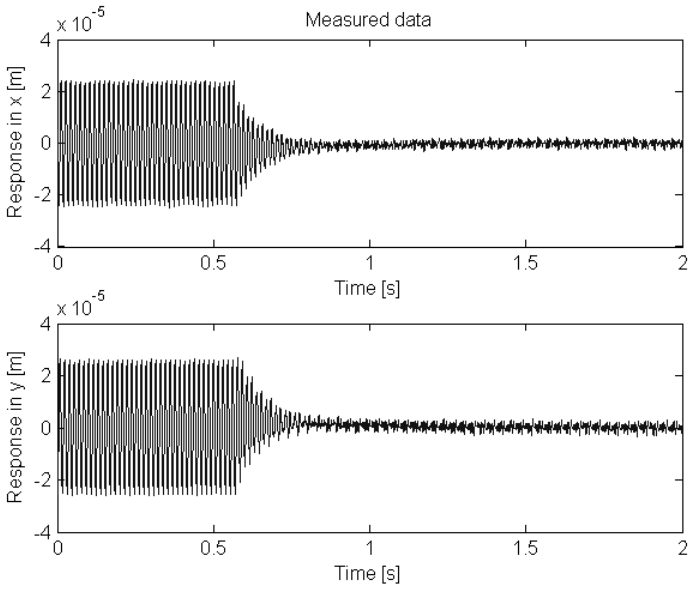

Figure 11. The responses were measured during the switch-on of the convergent control. The rotational speed was 65 Hz.

Next, the convergent control algorithm was running continuously and the rotational speed was swept. The sweep started from 11 Hz and ended to 65 Hz, its rate was 16.7 Hz/min (1000 rpm/min). The displacement response was approximately constant (about 2 microns, peak) over the operational range excluding two separate instants of time. The reason for these peaks was a discontinuity in the reference signals. The reference signals are used to generate the compensation force. The signals are multiplied with the Fourier coefficients computed in Equation (14) (see Figure 4). The Fourier coefficients adjust the gain and the phase of the compensation signal, but do not change the signal shape. For this reason, the compensation signal should be a sinusoid if a sinusoidal compensation force is wanted. The largest peak occurred due to the discontinuity was 64 microns.

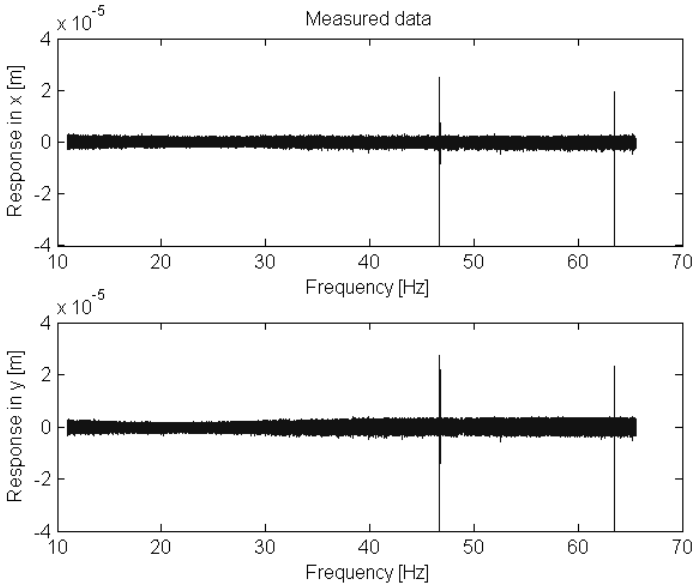

Figure 12. The responses were measured when sweeping the rotational speed from 11 Hz to 65 Hz with a rate of 16.7 Hz/min. Two peaks in each signal were due to discontinuities in the reference signal.

3.4 Responses in frequency domain

The displacement measurements shown in Figure 9, Figure 10, and Figure 11, were analysed in the frequency domain. The spectra (autopower, flattop window, 0.5 Hz resolution, 75 % overlap) were computed when the feedback control system was working alone and when both algorithms were working together. The results when run at 25 Hz are shown in Figure 13. The disturbance at the frequency of rotation was compensated by the convergent control algorithm. Similar behaviour is shown in Figure 14 and Figure 15, the rotational speed being 40 Hz and 65 Hz, respectively.

A peak at 97.5 Hz appeared in the spectra together with the use of convergent control. The magnitude of the peak was about 1 micron. The frequency of the peak was not dependent on the rotational frequency; or the rotor did not have a resonance in that region. The update frequency of the Fourier coefficients was considered as a potential reason for the peak. The update frequency was 97.7 Hz; *i.e.* the control unit was run at 9766 Hz and the coefficients were updated every 100th control period. The update frequency was changed to 49 Hz (every 200th period) and to 195 Hz (every 50th period) in order to confirm the assumption. The frequency of the peak was changed together with the update frequency. The same tests also indicated that lower update frequencies than about 100 Hz led to poor performance of the algorithm. The discussion concerns only the coefficient update frequency; the output of the convergent control was computed at a frequency of 9766 Hz.

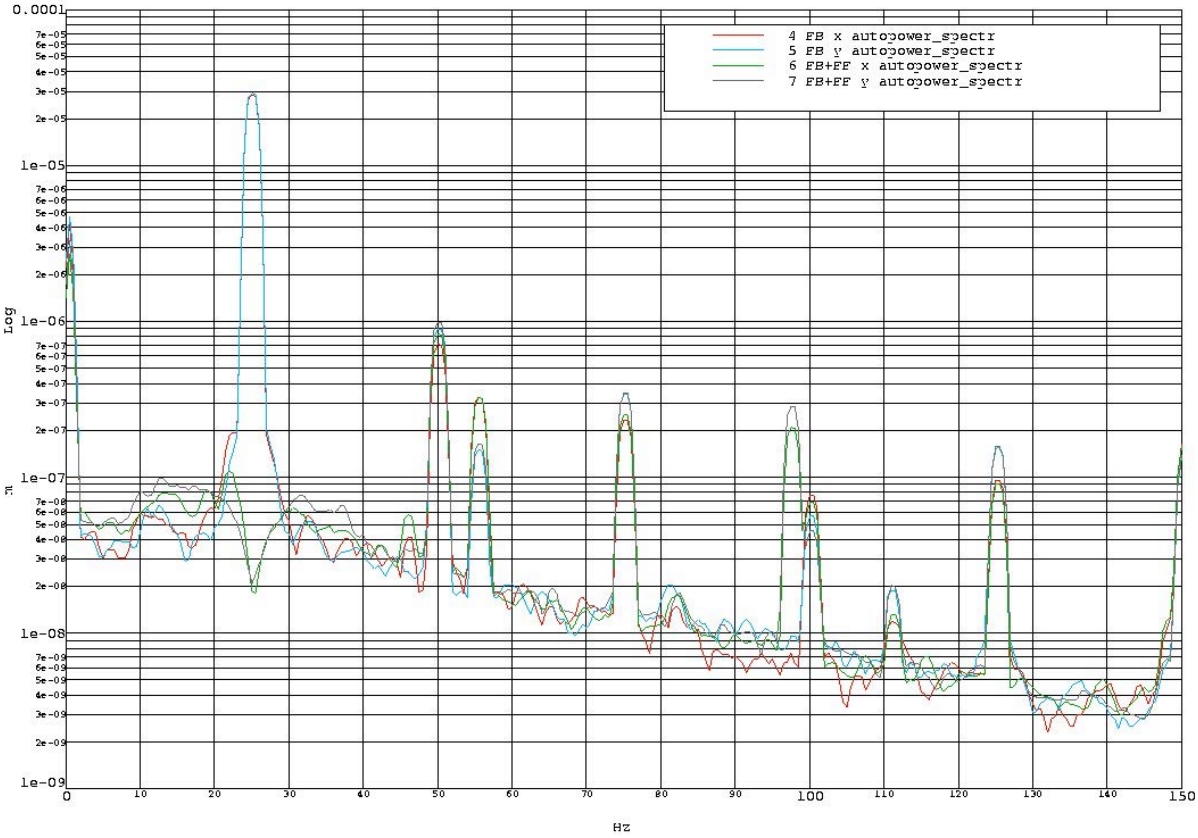

Figure 13. The spectra when the rotor was running at 25 Hz (FB: feedback control alone, FB+FF: both algorithms working).

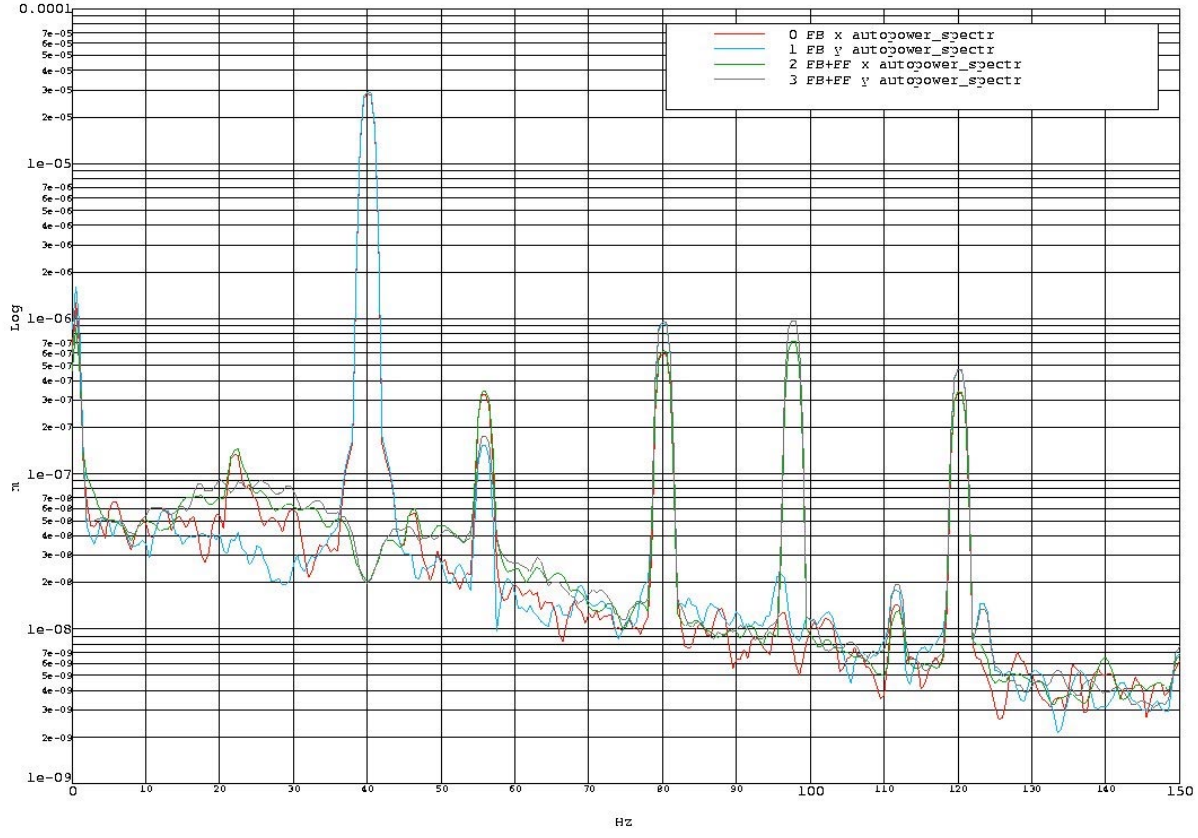

Figure 14. The spectra when the rotor was running at the critical speed, 40 Hz.

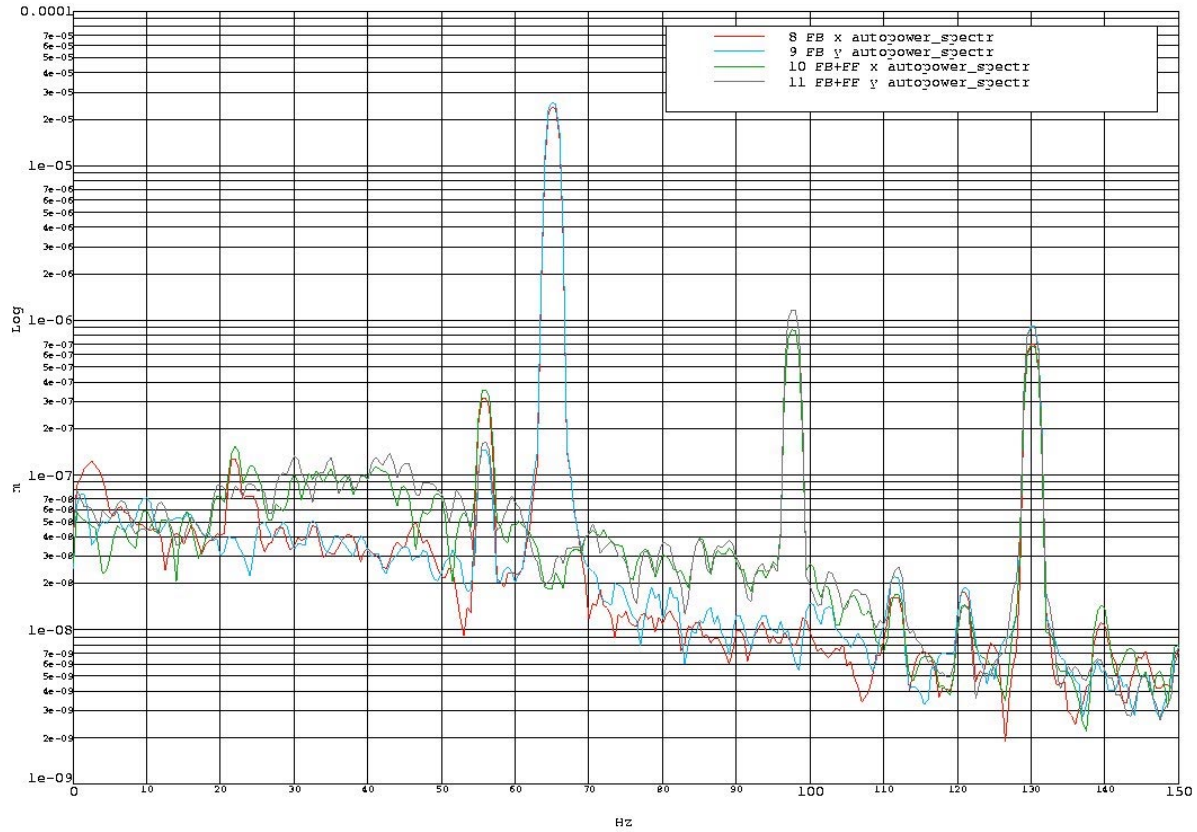

Figure 15. The spectra when the rotor was running 65 Hz.

3.5 Force commands

The force commands generated by the feedback and feedforward control loops were recorded with *Transient Recorder* tool in *AMBGui* program. The sampling rate was 9766 Hz. In Figure 16, the force commands when the rotational speed was 25 Hz are shown. First, the imbalance forces are to be compensated by the feedback control. When switched on, the feedforward control compensates the imbalance forces at the frequency of rotation. Figure 17 shows the force commands when operating at the critical speed (40 Hz). Figure 18 shows the commands when running 65 Hz. Note that the feedback control running alone and the feedback control running together with the feedforward control were not synchronously triggered. Hence, the phases between these measurements should not be compared. With the feedforward compensation running, the magnitude of the used forces remained approximately constant even the displacement was significantly less than obtained with the feedback control alone.

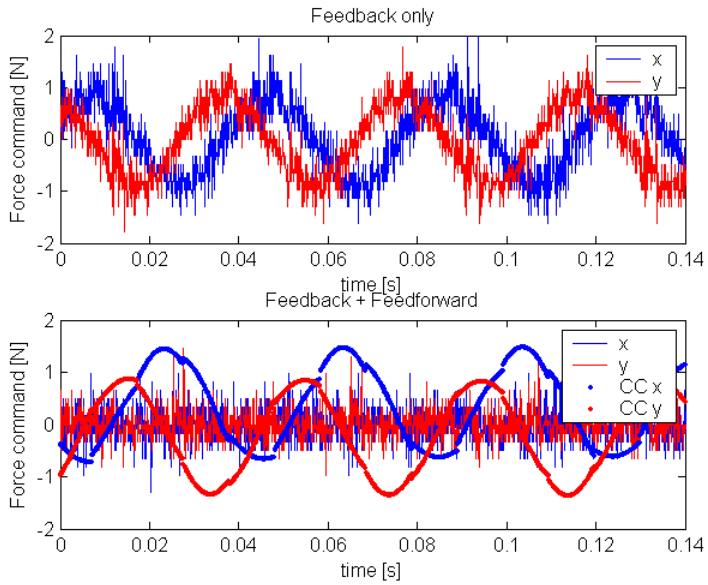

Figure 16. The force command signals generated when running feedback control alone was characterised by one sinusoidal signal (above). Feedforward control compensated the sinusoidal disturbance at the frequency of rotation (below). The rotational speed was 25 Hz.

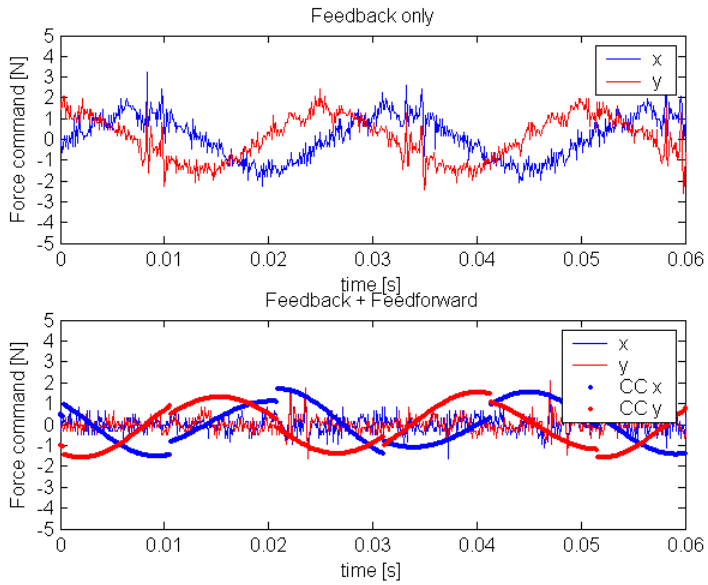

Figure 17. The force commands recorded when the rotational speed was 40 Hz. The discontinuous feedforward signal indicated the weakened quality of the reference signal.

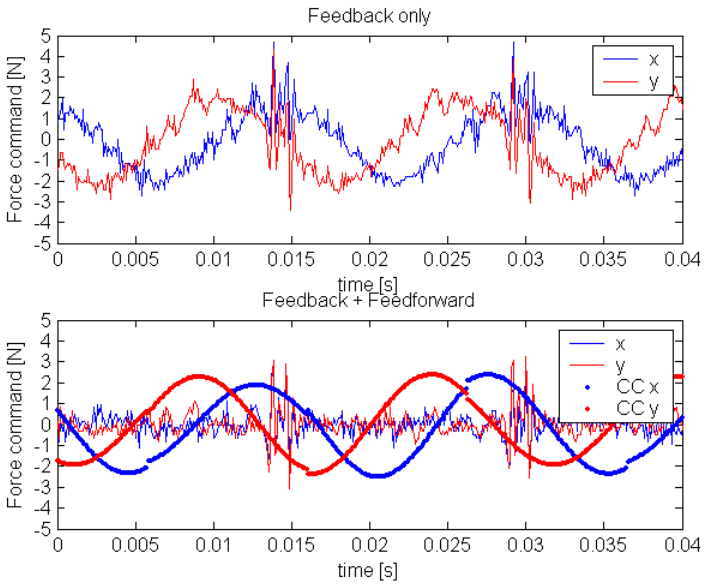

Figure 18. The force commands were also recorded when running 65 Hz.

The results indicated that discontinuities in the feedforward compensation signal caused peaks in feedback signal. Sometimes they were noticeable also in the displacement signal. Adjustment of the pulse sensor improved the quality of signals. Another set of measurements can be found in Appendix 3. They were recorded before the quality of the reference signal was improved. The results presented in Chapter 3 were acquired after the improvement of the reference signal.

4 Discussion

In simulations, both algorithms converged with disturbances from 10 Hz to 80 Hz. The convergence was fastest and smoothest around the resonance region, from 30 Hz to 50 Hz. At frequencies below resonance, the convergence was slower. This was probably because the algorithms need 'sufficient amount' of information for adaptation and the acquisition time of information is inversely proportional to the frequency. The simulations indicated the convergent control algorithm having smoother but slightly slower behaviour than the adaptive FIR filter with the filtered x-LMS algorithm. These results hold with the chosen parameter values. The sensitivity to parameter variation, noisy signal *etc.* was not studied.

The FIR filter required significantly more computational power than the convergent control due to its high order. In principle, the FIR filter should not require such a high order to compensate a disturbance at one frequency. Two filter coefficients per frequency should be sufficient (Fuller *et al.* 1996). However, the tests indicated that one has then to select the update frequency carefully. The proper selection of the FIR filter coefficients requires further studies. The order of the FIR filter may have an effect on convergence and vibrating response because the modes of the filter were not persistently excited.

In the experiments, the convergent control algorithm worked from 11 Hz to 65 Hz. The lower limit was set by the availability of the reference signal. The higher limit was selected as a frequency clearly above the critical speed at 40 Hz. After the convergent control algorithm was switched on the response decreased to order of two microns. When the feedback control was running alone the displacement was about 30 microns (peak). The algorithm reached the

steady-state condition in about 0.25 seconds after switched on. As in the simulations carried out in this study, the convergence was found smooth. The convergence was fast and smooth when compared with the results on the FIR filter, presented in Tammi (2003).

A discontinuous reference signal caused transients in responses. For a short moment, the rotor was deflected from its orbit until the feedback control restored the situation. Similar effects were observed when testing the adaptive FIR filter in Tammi (2003). The convergent control helped to trace the cause. In the convergent control, the compensation signal is derived immediately from the reference signal. Thus, the current input of the reference signal directly affects the next output. Whereas in the adaptive FIR filter, the compensation signal is a weighted average of the compensation signal samples. In other words, a single input sample does affect the output alone in the adaptive FIR filter. For this reason, minor discontinuities may not be visible in the compensation signal. The convergent control algorithm used in this study may be more sensitive to imperfections in the reference signal than an adaptive FIR filter of a high order.

The vibrations were amplified at about 100 Hz when feedforward control was used. With feedforward control, the magnitude of the peak at 97.5 Hz was an order of 1 micron. With feedback control only, no peak appeared. This behaviour was caused by the Fourier coefficient update. The reason requires deeper study of the convergent control dynamics.

References

Fuller C.R., Elliot S.J., Nelson P.A. *Active control of vibration*. Academic Press. London. 1996. 332 p. ISBN 0-12-269440-6.

Hall, S.R. & Wereley, N.M., 1989. *Linear control issues in the higher harmonic control of helicopter vibrations*. Proc. 45th Annu. Forum Amer. Helicopter Soc. (Boston, MA), May 1989. pp. 955-971.

Järviluoma M. & Valkonen A. *Test equipment and controller for active rotor vibration damping*. Progress report. VTT Automation. Oulu. 2001. 38 p.

Järviluoma M. & Valkonen A. *Test equipment and controller for active rotor vibration damping: set-up, methods, results*. Progress report. VTT Automation. Oulu. 2002. 53 p.

Järviluoma M. *Control algorithms for active rotor vibration damping, repetitive and related control methods*. VTT Electronics, VTT Industrial Systems. 2003.

Knospe C.R., Fedigan J., Hope R.W., Williams R.D. *A multitasking DSP implementation of adaptive magnetic bearing control*. IEEE Transactions on control systems technology. Vol 5. No 2. March 1997. pp. 230-238.

Lantto E. *Robust control of magnetic bearings in subcritical machines*. Acta Polytechnica Scandinavica. EL 94. ESPOO 1999. 143 p. ISBN 952-5148-80-7.

Sievers L.A. & von Flotow A.H. *Linear control design for active vibration isolation of narrow band disturbances*. Decision and Control, 1988. Proceedings of the 27th IEEE Conference on.1988. vol.2. pp. 1032 -1037.

Tammi K. *Active vibration control of rotor - test environment with non-contact magnetic actuator*. Smart materials and structures. VTT Symposium 225. VTT - Technical Research Centre of Finland. Espoo. 2003. pp 67-80. ISBN 951-38-6278-X. ISSN 0357-9387.

Appendix 1

Figure 1 shows the simulation model used. Both algorithms were implemented in the same simulation model. The convergent control used a cosine and a sine signal as the reference signals while the FIR filter used a sine. The disturbance of the same frequency as the references was fed into the outputs of the systems. The algorithms functioned in the 'Matlab function' blocks. They were realised as m-files shown in Table 1.

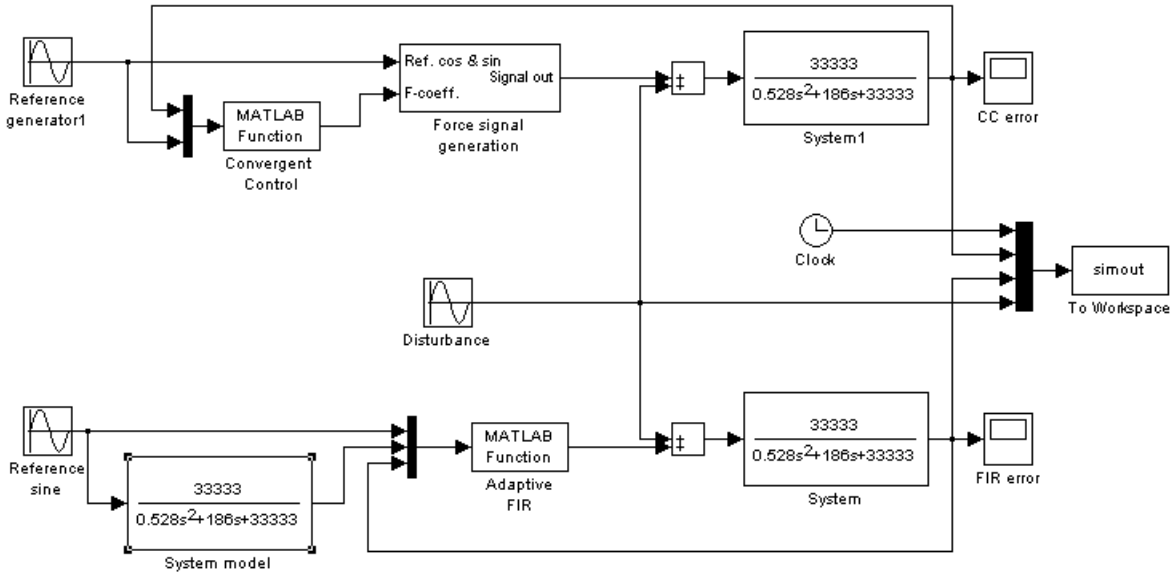

Figure 1. The Simulink model consisted of the convergent control (above) and the FIR filter (below) branches.

Table 1. The contents of m-files used are shown below.

Initialisation

```
function init_sim();
clear all;
global freq;
freq = 10;

% For Convergent control
global U_old;
U_old = 0;
global a_cc;
a_cc = 0.02;

% For adaptive FIR
global order;
global alpha;
global h;
global ref_seq;
global input_seq;

order = 50;
alpha = 0.002;
h = zeros(order,1);
ref_seq = zeros(order,1);
input_seq = zeros(order,1);
```

Convergent Control

```
function U = conv_control(err,ref_co,ref_si)

% Computes Convergent control output from
system output and reference cosine & sine

% Remember run init_sim first
global U_old;
global freq;
global a_cc;
% Complex correlation with reference signal
X = 2 * err * (ref_co - i * ref_si);

% Model inverse, A = ((T'T)^-1)T'
w = i * 2 * pi * freq;
T = 33333/(0.528 * w^2 + 186 * w + 33333);
A = - a_cc * inv(conj(T) * T) * conj(T);

% Covergent control update law
U = U_old + A * X;

% Save old control output
U_old = U;
```

FIR filter

```
function out = fir_filter(signal_in,reference,error)

% Adaptive FIR filter

global order;
global alpha;
global h;
global ref_seq;
global input_seq;

% Update signal sequence
for I = 1:(order - 1)
   input_seq(order-I+1) = input_seq(order-I);
end
input_seq(1) = signal_in;

% Update reference sequence
for I = 1:(order - 1)
   ref_seq(order-I+1) = ref_seq(order-I);
end
ref_seq(1) = reference;

% Update FIR coefficients
h_old = h;
h = h_old - alpha .* error .* ref_seq;

% Compute FIR output
out = h'* input_seq;
```

Appendix 2

Table 1. The convergent control code was implemented in C-language on the DSP environment.

```
// Correlation measurement in X-direction, real and imaginary parts
corr_meas[0] = 2*elem_signals_for_c[2]*position_error[0]*cc_on; // Real part = cos * err
corr_meas[1] = 2*elem_signals_for_c[3]*position_error[0]*cc_on; // Imaginary = -sin * err

// Correlation measurement in Y-direction
corr_meas[2] = 2*elem_signals_for_c[2]*position_error[1]*cc_on; // Real part = cos * err
corr_meas[3] = 2*elem_signals_for_c[3]*position_error[1]*cc_on; // Imaginary = -sin * err

// Integrate over n samples then reset and set new correlation values
if (integr_counter < 10000)
{
                        // X-dir.
                        integr_corr_meas[0] = integr_corr_meas[0] + corr_meas[0];
                        integr_corr_meas[1] = integr_corr_meas[1] + corr_meas[1];

                        // Y-dir.
                        integr_corr_meas[2] = integr_corr_meas[2] + corr_meas[2];
                        integr_corr_meas[3] = integr_corr_meas[3] + corr_meas[3];
}

if (integr_counter > 9999) // Conv Control and integrator reset after n samples, results is moved to hold
{
                        // X-dir. Gain 1/n over n periods
                        curr_corr[0] = 0.0001*integr_corr_meas[0];
                        curr_corr[1] = 0.0001*integr_corr_meas[1];

                        // Y-dir.
                        curr_corr[2] = 0.0001*integr_corr_meas[2];
                        curr_corr[3] = 0.0001*integr_corr_meas[3];

                        // Compute model inverse: real and imaginary parts at each speed
                        angular_freq = 6.2831853*rotation_freq; // 2*pi*f
                        model_inverse[0] = cc_gain*(4.66662 - 0.00007392*angular_freq*angular_freq); // m*(i*w)^2 + k
                        model_inverse[1] = -cc_gain*0.02604*angular_freq; // c*i*w

                        // Convergent Control in X-direction U(k+1) = U(k) + A(w) * X(k). 0: real, 1: imag
                        // Use of _direct_ correlation value. ADDED 12.2.2003!
                        U_new[0] = leak*U_old[0] + model_inverse[0]*corr_meas[0] - model_inverse[1]*corr_meas[1];
                        U_new[1] = leak*U_old[1] + model_inverse[1]*corr_meas[0] + model_inverse[0]*corr_meas[1];

                        // Y-direction. 0 & 2: real, 1 & 3: imag
                        U_new[2] = leak*U_old[2] + model_inverse[0]*corr_meas[2] - model_inverse[1]*corr_meas[3];
                        U_new[3] = leak*U_old[3] + model_inverse[1]*corr_meas[2] + model_inverse[0]*corr_meas[3];

                        // Save new values for next period
                        U_old[0] = U_new[0];
                        U_old[1] = U_new[1];
                        U_old[2] = U_new[2];
                        U_old[3] = U_new[3];
```

```
                    // Reset integrator
                    integr_corr_meas[0] = 0;
                    integr_corr_meas[1] = 0;
                    integr_corr_meas[2] = 0;
                    integr_corr_meas[3] = 0;
                    integr_counter = 0;
}
integr_counter++;

// Realise time signals according force commands U(k)
cc_time_signal[0] = U_new[0]*elem_signals_for_c[2] + U_new[1]*elem_signals_for_c[3];
cc_time_signal[1] = U_new[2]*elem_signals_for_c[2] + U_new[3]*elem_signals_for_c[3];

// Output is computed if add_forces <> 0
cc_output[0] = add_forces*cc_time_signal[0];
cc_output[1] = add_forces*cc_time_signal[1];

return 0;
}
```

Appendix 3

This appendix is to show the problems caused by discontinuities in the reference signals used by convergent control. The measurement of the rotational speed was unsettled. The fluctuation in the rotational speed measurement was observed from the reference signals and the rotational speed indicator. The adjustment of the pulse sensor (phasor) probe decreased the fluctuation. The time records to be presented here were obtained before the adjustment.

The force commands were recorded at three constant speeds: 25 Hz, 40 Hz and 65 Hz (Figure 1, Figure 2 and Figure 3). In each figure, the plot above shows the force commands with the feedback control running alone. The force commands derived by the feedback and feedforward control together are shown in the plot below. When the feedback control was running alone, the force commands were characterised by a sinusoidal signal due to the excitation at the speed of rotation. The feedforward compensation, when switched on, compensated the disturbance at the frequency of rotation.

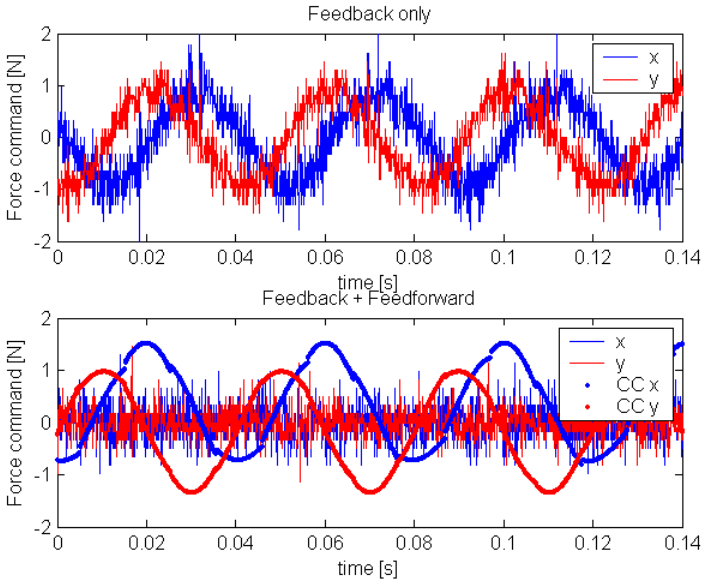

Figure 1. The force command when running at 25 Hz.

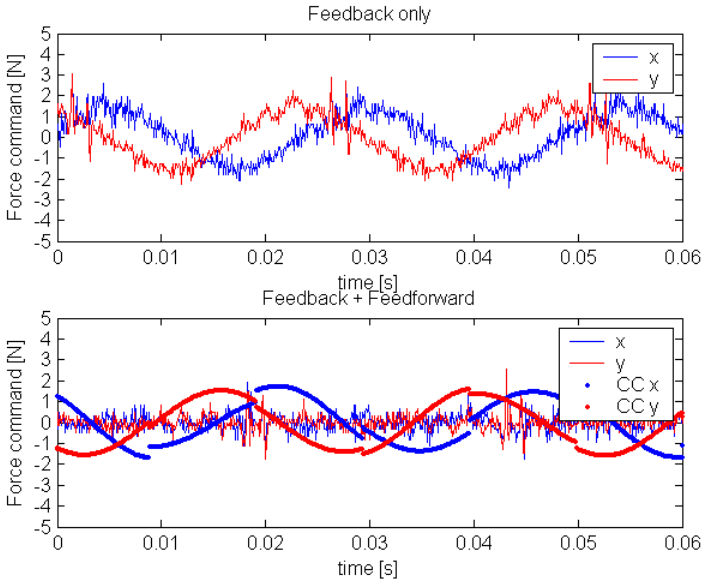

Figure 2. The force command when running at 40 Hz (critical speed).

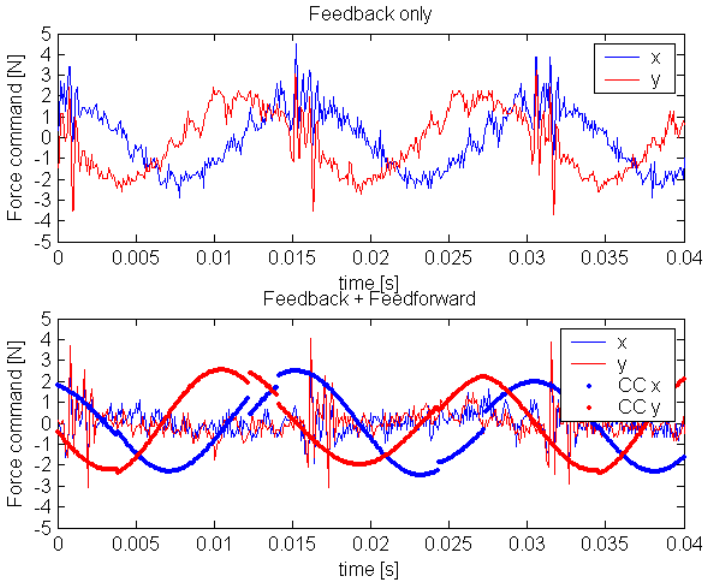

Figure 3. The force command when running at 65 Hz.